

A Regression Based Hourly Day Ahead Solar Irradiance Forecasting Model by Labview using Cloud Cover Data

Oğuzhan Ceylan¹, Michael Starke², Phil Irminger², Ben Ollis², Kevin Tomsovic¹

¹ Dept. of Electrical Engineering and Computer Science
The University of Tennessee
oceylan@utk.edu, tomsovic@utk.edu

² Power & Energy Systems Group
Oak Ridge National Laboratory
starkemr@ornl.gov, irmingerp@ornl.gov, ollistb@ornl.gov

Abstract

This paper applies a regression based numerical method for photovoltaic power output hourly forecast. The method uses a historical data composed of irradiance, azimuth, zenith angle and time of day information. In every run of the forecast program, publicly available cloud cover forecast data for the following day is obtained, and by using a numerical regression based method a function is fit. Then by using the publicly available temperature forecast data, forecasted irradiance data, and computed solar position (zenith, azimuth) data, both power output and temperature module output of PV array is computed. Numerical forecast results show that, they are in accordance with the actual data.

1. Introduction

With the evolution to smarter electrical power grids, the usage of photovoltaic technologies are increasing. Since world's energy need is projected to be 30 TW in 2050 (which is triple times of the usage in 2011), to stabilize the CO_2 in atmosphere, the ratio of photovoltaics (PVs) and renewables will increase [1]. The efficiency of technology of solar cells is developing day by day and the costs are reducing, this also motivates the industry to use more and more PVs in the near future. However, different from conventional power plants, power output of PVs are not constant in time, their fluctuated behavior of the power outputs are due to intermittent nature of the irradiance, and hence due to the change in cloud covers. The impacts of solar penetration into power systems is detailly discussed in [2].

This work was sponsored by the Office of Electricity Delivery & Energy Reliability, U.S. Department of Energy under Contract No. DE-AC05-00OR 22725 with UT-Battelle and conducted at ORNL and UT Knoxville. This work also made use of Engineering Research Center Shared Facilities supported by the Engineering Research Center Program of the National Science Foundation and the Department of Energy under NSF Award Number EEC-1041877 and the CURENT Industry Partnership Program. The first author would like to thank the Scientific and Technological Research Council of Turkey (TUBITAK) for its financial support. Oğuzhan Ceylan and Kevin Tomsovic are with the Department of Electrical Engineering and Computer Science, The University of Tennessee (UT), Knoxville, TN 37996 USA (email: oceylan@utk.edu; tomsovic@utk.edu) Michael Starke, Philip Irminger and Ben Ollis are with the Oak Ridge National Laboratory (ORNL), Oak Ridge, TN 37831 USA (email: starkemr@ornl.gov; irmingerp@ornl.gov, ollistb@ornl.gov).

PV outputs need to be forecasted as accurate as possible to obtain an efficient operation in electrical power systems.

Several methods have been used in PV power output forecasting. One of these methods is time series modeling [3]. In [4] power output of PV system is forecasted by using artificial neural networks. The article in [5] predicts hourly forecast using artificial neural networks and wavelet transform together. Genetic algorithm provides the best simulation results in [6] when used with artificial neural networks. In [7] Kalman Filters are used for forecasting. Another tool used to forecast power outputs of PV Systems is support vector machines [8, 9]. Detailed information on solar irradiance forecasting methods may be found in [10].

According to [10] global horizontal irradiance (GHI) forecasting approaches may be applied from very short timescale from 5 min to 6 hours where artificial neural networks, autoregressive and autoregressive moving average models are used. For irradiance forecasting information of cloud cover is needed. This may be either found in satellite images, or ground based sky images. The work [11], that uses cloud motion vectors from satellite images show good performance for periods from 30 minutes to 6 hours ahead. Ground based sky images may be used for very short term irradiance forecasting [12].

This study presents a computational approach to forecast PV outputs by using a numerical regression method. Since the solar irradiance of an area is based on the positions and angles (longitude, latitude, azimuth, zenith), these components are involved in forecasting processes. The method uses publicly available daily hour based cloud cover forecast data, and temperature forecast data. Different from a previous work [13], where neural network is used in forecasting phase, a numerical regression algorithm is applied. After obtaining next day's forecasted irradiance values, the model uses Newton Raphson model based MPPT program for PV power output calculation. PV module temperature model uses publicly available temperature forecasts, together with the calculated power output forecasts. Labview is used as the programming environment.

The rest of the paper is organized as follows. The second section explains the model for PV power output and module temperature forecast model. The subsections of this section briefly explain the data preparing and calculation processes in the model. Final section illustrates the test results and compares these results to the actual ones.

2. The Model

A model is developed for PV panel power output and module temperature forecast in Labview. The flowchart of the model is shown in Figure (1). In order to forecast the outputs of the next day, the first step is to collect cloud cover data from web. Then by using the longitude, latitude information of the current location, a function that calculates the azimuth, and zenith angles of each hour in the net day is called. With these data and the historical data composed of azimuth, zenith, hour of day and cloud cover data, irradiance values are forecasted by using a numerical regression algorithm. Final step includes the calculation of MPPT and module temperature by using the calculated irradiance forecasts and temperature forecasts obtained from web. The labview snapshot of the main program is also given in Figure (2). The following subsections briefly describe these steps.

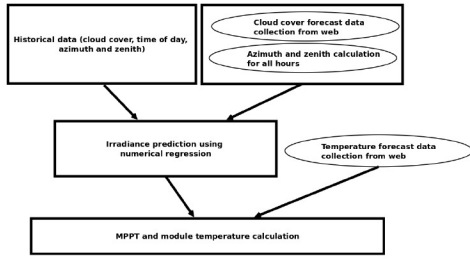


Figure 1. Flowchart of PV power output and module temperature forecast model

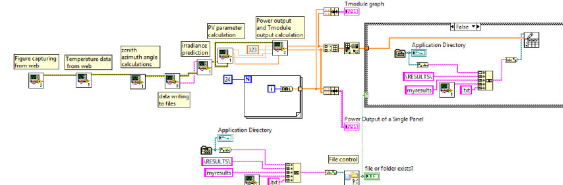


Figure 2. Labview PV power output and module temperature forecast program

2.1. Cloud Cover Data Collection

Cloud cover forecast data is obtained from publicly available data from web [14]. Figure 3 shows a forecasted satellite image of South East part US. The coordinates of Oak Ridge where DECC Lab is located is known and is represented with a black star on the image. On the right hand side of the image, the legends show the colors and their cloud cover percentage equivalents. The process for finding the cloud cover forecast data for the next day is as follows:

- Connect to the cloud cover forecast webpage.
- Automatically download the cloud cover forecast images to the computer that runs the forecasting program.
- By using the coordinate information of ORNL DECC Lab, find the corresponding pixel values, and compare to the legend colors which specify the cloud cover percentages for each image, and obtain cloud cover percentage values, and store these values.

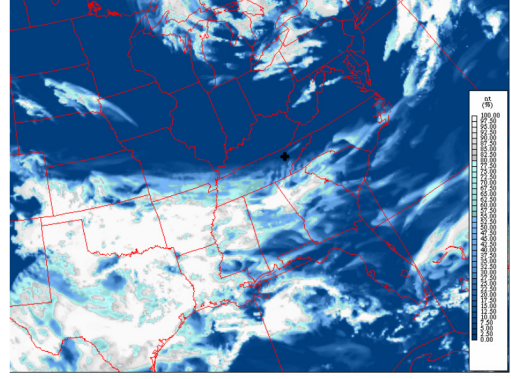


Figure 3. A sample cloud cover image of US South East, and the position of ORNL DECC Lab.

2.2. Azimuth and zenith angle calculation

A matlab function based on [15] written by Vincent Roy was translated into Labview. The function uses year, month, day, hour, minute, second, difference from Greenwich time, latitude, longitude, and altitude of the location as inputs. The outputs of the function are zenith and azimuth angles in degrees. For each day to be forecasted, the function is run with one hour intervals.

2.3. Irradiance Forecast Using Numerical Regression

Forecasting irradiance includes two steps. The first step uses the historical data, and the second step forecasts the irradiance values with the help of historical data and uses a numerical regression based model, where the historical information is fit into the forecasted function values.

2.3.1. Historical Data

A dataset consists of actual values of time of the day, cloud cover forecasts, azimuth and zenith angles for 40 days was used.

2.3.2. Irradiance Forecasting

Since, the behavior of the irradiance output is very complex, a function composed of linear and non-linear components was used to fit the historical data. The function used for fitting the data is given below:

$$\begin{aligned}
 F = & \alpha_1 + \alpha_2 \times e^{\frac{t}{50}} \times \sin(t) + \alpha_3 \times c + \alpha_4 \times z + \alpha_5 \\
 & \times a + \alpha_6 \times t^2 + \alpha_7 \times z^2 + \alpha_8 \times t + \alpha_9 \times \cos(c) \\
 & + \alpha_{10} \times z \times \sin(t) + \alpha_{11} \times a \times \sin(t)^2 + \alpha_{12} \\
 & \times e^{\frac{t}{100}} \times \sin(t) + \alpha_{13} \times e^{\frac{a}{100}} \times \sin(t) + \alpha_{14} \\
 & \times e^{\frac{z}{100}} \times \sin(c) + \alpha_{15} \times e^{\frac{a}{100}} \times \sin(c) + \alpha_{16} \\
 & \times c \times \sin(t) + \alpha_{17} \times z \times t + \alpha_{18} \times z \times c \\
 & + \alpha_{19} \times e^{\frac{z}{100}} \times \cos(t) + \alpha_{20} \times e^{\frac{a}{100}} \times \cos(t) \\
 & + \alpha_{21} \times e^{\frac{z}{100}} \times \cos(c) + \alpha_{22} \times e^{\frac{a}{100}} \times \cos(c) \\
 & + \alpha_{23} \times \sin(z) + \alpha_{24} \times \sin(a) + \alpha_{25} \times e^{\frac{z}{100}} \\
 & \times \tan(t) + \alpha_{26} \times \cos(z)^2 + \alpha_{27} \times \cos(a)^2 \\
 & + \alpha_{28} \times e^{\frac{a}{100}} \times \cos(c)^2 + \alpha_{29} \times e^{\frac{a}{100}} \times \cos(t)^2 \quad (1)
 \end{aligned}$$

where, t , c , a , z , represent time, cloud cover, azimuth and zenith respectively. The algorithm for forecasting the next day's irradiance values can be given as follows:

- For all data points of 40 days, calculate the value of the following function, and store it in a vector \mathbf{V} .

$$\begin{aligned}
 F &= 1 + e^{\frac{t}{50}} \times \sin(t) + c + z + a + t^2 + z^2 + t \\
 &+ \cos(c) + z \times \sin(t) + a \times \sin(t)^2 + e^{\frac{z}{1000}} \\
 &\times \sin(t) + e^{\frac{a}{100}} \times \sin(t) + e^{\frac{z}{100}} \times \sin(c) \\
 &+ e^{\frac{a}{100}} \times \sin(c) + c \times \sin(t) + z \times t + z \times c \\
 &+ e^{\frac{z}{100}} \times \cos(t) + e^{\frac{a}{100}} \times \cos(t) + e^{\frac{z}{100}} \times \\
 &\cos(c) + e^{\frac{a}{100}} \times \cos(c) + \sin(z) + \sin(a) \\
 &+ e^{\frac{z}{100}} \times \tan(t) + \cos(z)^2 + \cos(a)^2 \\
 &+ e^{\frac{a}{100}} \times \cos(c)^2 + e^{\frac{z}{100}} \times \cos(t)^2 \quad (2)
 \end{aligned}$$

- Calculate the α coefficient vector as follows:

$$\alpha = (V' \times (V))^{-1} \times V' \times G \quad (3)$$

where G is a vector whose elements consists of the actual irradiance values for 40 days of data.

- Using the computed α values and the function given above predict next day's irradiance values using equation 1.

2.4. Temperature forecasts

Temperature forecasts are performed by getting data from [16]. The process starts by computing the number of days from the beginning of the current year, and that day's forecast data webpage is reached from labview, and the code of the page is assigned to a string variable. Specific hour temperature values are sought in this string in a systematical way and then by using interpolation next day's temperature forecasts are obtained. A sample temperature forecast webpage that is used in obtaining data is shown in Figure (4).

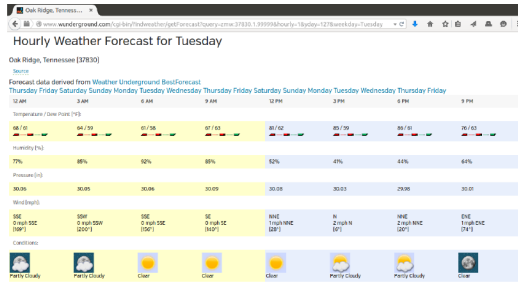


Figure 4. A sample temperature forecast webpage

2.5. MPPT and Module Temperature Calculation

The model in [17] was used for MPPT calculation. This model uses an PV circuit model comprises of a diode, series and parallel resistances as shown in Figure (5).

The current of the pv module is computed by using Kirchoff's law. Numerically, this process requires subtracting the sum of diode current and the current passing through parallel

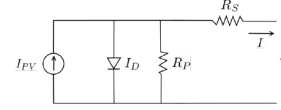


Figure 5. Single diode PV representation

resistance from the photovoltaic current as represented in equation (4):

$$I = I_{pv} - I_0 \left[e^{\frac{V + R_s I}{V_t \alpha}} - 1 \right] - \frac{V + R_s I}{R_p} \quad (4)$$

where, I_{pv} and I_0 are the photovoltaic and saturation currents of the PV array respectively. $V_t = N_s k T$ is the thermal voltage (with N_s cells in series connection), R_s and R_p are equivalent series and parallel reactances, α is diode constant whose typical value lies between 1 and 1.5.

2.5.1. Determining R_s , R_p , P_{max} , I_{pvmax}

Several parameters such as: K_v open circuit voltage temperature coefficient, K_I short-circuit current temperature coefficient, $V_{oc,n}$ nominal open circuit voltage, $I_{sc,n}$ nominal short circuit current, V_{mp} voltage at the maximum power point, I_{mp} current at maximum power point are known. Other constants are: k Boltzmann constant, q electron charge. Several parameters of 280W Hanwa Solar PV are given in Table (1), [13]:

Table 1. HSL72 Solar PV Module Parameters

| Definition | Value |
|--------------------------------------|--------------|
| Maximum Power (P_{max}) | 280 W |
| Voltage at MP (V_{mp}) | 35.7 V |
| Current at MP (I_{mp}) | 7.84 A |
| Voltage at Open Circuit (V_{oc}) | 44.6 V |
| Current at Open Circuit (I_{sc}) | 8.43 A |
| K_i | 0.005058 A/K |
| K_v | -0.14718 V/K |
| N_s | 72 |

In the computations, diode saturation current given below is also used:

$$I_0 = \frac{I_{sc,n} + K_I \Delta T}{e^{\frac{V_{oc,n} + K_V \Delta T}{\alpha V_t}} - 1} \quad (5)$$

where $\Delta T = T - T_n$, represents the difference between the ambient and the nominal temperature, hence the temperature has an effect on diode saturation current.

The process for determining the serial and parallel reactances, maximum power and maximum photovoltaic current starts with initially setting R_s to 0, and R_p to $\frac{V_{mp}}{I_{sc,n} - I_{mp}} - \frac{V_{oc,n} - V_{mp}}{I_{mp}}$. Then by selecting stepsize of R_s a small step value such as 0.003, R_s is slowly increased, and in each step following operations are performed:

$$I_{pv,n} = \frac{R_p + R_s}{R_p} I_{sc,n}. \quad (6)$$

$$I_{pv} = (I_{pv,n} + K_i \Delta T) \frac{G}{G_n} \quad (7)$$

where G is the actual irradiance, G_n is the nominal irradiance.

$$R_p = \frac{V_{mp}(V^-)}{V_{mp}I_{pv} - V_{mp}I_o e^{\frac{V^-}{aNs} - \frac{q}{kT}} + V_{mp}I_o - P_{max}} \quad (8)$$

where $V^- = (V_{mp} + I_{mp}R_s)$ Equation (4) is solved for all V values from 0 to $V_{oc}N_{ser}$, by using Newton Raphson method and for each V value, an I value is obtained, hence all the power values for these pairs may be computed. Maximum power value is computed and stored.

From all the maximum powers, there is only one point that satisfies the condition $P_{max,m} = V_{mp}I_{mp}$ at the (V_{mp}, I_{mp}) point [17]. By using this, $P_{max} = 6719.82$, position=102, $R_s = 0.306$, $R_p = 573.791$, $I_{pvmax} = 8.47345$ are found. The graph of P_{max} as a function of R_s is shown in Figure 6.

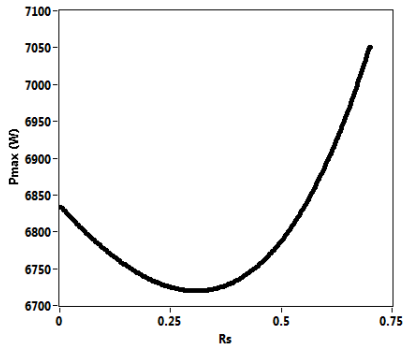


Figure 6. P_{max} , R_s graph.

2.5.2. Calculation of PV Power Output

PV Power Output calculation uses R_p , R_s , I_{pvmax} , ambient temperature T , and irradiance G as inputs. P and T_{module} are the outputs.

A thermal calculation model for a PV module is given in [18]. This model takes the decrease and increase in the temperatures into consideration for module temperatures. The change in module temperature is given by the following equation:

$$C_{module} = q_{lw} + q_{sw} + q_{conv} - P_{out} \quad (9)$$

where, C_{module} , q_{lw} , q_{sw} , q_{conv} , and P_{out} represent, the heat capacity of the module, short wave heat transfer, convection heat transfer, and power generated by the module respectively. Detailed information on these equations may be found in [18].

The algorithm for calculation of PV Power output and module temperature is given in Algorithm 1. As can be seen below, the algorithm includes a main loop for 24 hour simulation and two separate loops. The first separate loop performs PV power output calculation by using Newton Raphson method, and the second separate loop calculates temperature module by using Euler Method.

3. Tests and Results

The proposed method is tested from 24th to 30th of June 2015. Obtained simulation results are compared to the actual values obtained from the PV module installed on ORNL DECC Lab. In Figure (7) the actual and forecasted irradiance values for the specified days are illustrated. As can be seen from the figure, the actual results and the forecasted results for the days with

Algorithm 1 PV output and temperature module calculation algorithm

Inputs: R_p , R_s , I_{pvmax} , T , G

Outputs: I , V , P , T_{module}

for Day of Time=1:23 **do**

for $V = 0 : V_{oc,n}Ns$ **do**

Inputs: R_p , R_s , I_{pvmax} , T , G

Outputs: I , V , P

Solve equation 4 with Newton Raphson Method using numerical derivatives: That is $I_{i+1} = I_i - \frac{f(I)}{f'(I)}$ and

$f'(I) = \frac{f(I+h)-f(I)}{h}$ where h is a small number.

From each V , I pairs find P_{max}

end

for Time = 0 : 3600s **do**

Inputs: G , $T_{ambient}$, P

Outputs: T_{module}

Solve equation 9 by using Euler Method. That is $T_{module(i+1)} = T_{module(i)} + \text{step}f'(T_{module(i)})$ and $f'(T_{module}) = \frac{f(T_{module}+h)-f(T_{module})}{h}$ where, step is a user defined step number and h is a small number.

end

end

less cloudy days are complying more comparing to the cloudy days. It is seen from the figure that highest irradiance error is obtained for 39th of June, the reason of this might be either the cloud cover forecast errors or irradiance measurement errors. The RMSE (root mean square error) and nRMSE(normalized root mean square error) value for 7 days irradiance simulation is calculated as 141.83 W/m^2 , and 0.45 respectively.

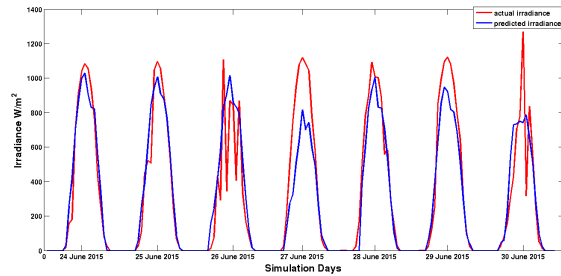


Figure 7. Actual and forecasted irradiance values for 24th to 30th of June 2015

Figure (8) illustrates the actual and forecasted power output of a single PV panel. Again the power output forecasts of PV panel are in compliance with the actual results. The errors increase for the days that have more fluctuations in power outputs. Since, the model uses, forecasted values in forecasting, this may also increase the errors in simulations. The RMSE and nRMSE values for power outputs is found as 1252.41 Watt and 0.9984 respectively.

Figure (9) shows the actual and forecasted temperature values of PV module. It is seen from the figure that the forecasted module temperatures catch the behavior of the actual module temperature values. The RMSE and nRMSE values for module temperature for one week is computed as 7.96 Celsius and 0.2514 respectively.

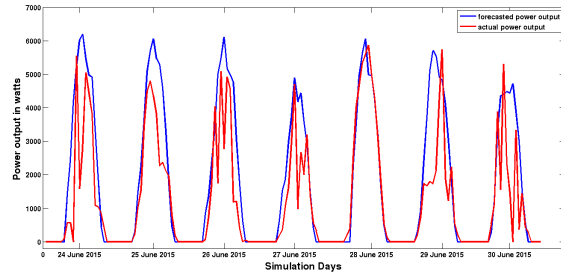


Figure 8. Actual and forecasted power output values for a single panel from 24th to 30th of June 2015

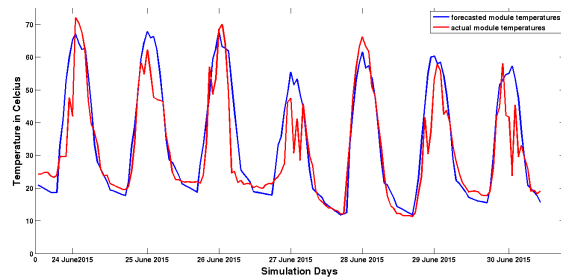


Figure 9. Actual and forecasted irradiance values for 24th to 30th of June 2015

4. Conclusion

This paper uses numerical regression method for PV output and module temperature output forecasting. The computation model uses publicly available cloud cover forecast information, and temperature forecast data and uses them in the forecasting process together with position and angle components such as longitude, latitude, azimuth, zenith. Labview is used for simulation tool. A sample of one week simulation results show that the irradiance, power, and module temperature forecasting results are in compliance with the actual results. In the future these forecast values are planned to be used in a microgrid operation and control environment.

5. References

- [1] T. M. Razykov, C. S. Ferekides, D. Morel, E. Stefanakos, H. S. Ullal and H. M. Upadhyaya, "Solar photovoltaic electricity: current status and future prospects", *Solar Energy*, vol. 85:8, pp. 1580–1608, August 2011.
- [2] D. Lew, N. Miller, K. Clark, G. Jordan, Z. Gao, "Impact of high solar penetration in the western interconnection." *Technical Report, National Renewable Energy Laboratories NREL/TP-5500-49667*, 2010
- [3] P. Bacher, H. Madsen, and H. A. Nielse, "Online short-term solar power forecasting", *Solar Energy*, vol. 83:10 pp. 1772–1783, 2009
- [4] M. Ding, L. Wang, and R. Bi, "An ANN based approach for forecasting the power output of photovoltaic system",

Procedia Environmental Sciences, vol. 11 pp. 1308–1315, 2011

- [5] P. Mandal, S. T. S. Madhira, A. U. I. Haque, J. Meng, R. L. Pineda, "Forecasting power output of solar photovoltaic system using wavelet transform and artificial intelligence techniques", *Procedia Comput. Sci.* vol.12, 332-337 2012.
- [6] H. T. C. Pedro, C. F. M. Coimbra, "Assessment of forecasting techniques for solar power production with no exogenous inputs", *Solar Energy* vol.86 , pp. 2017–2028 2012
- [7] S. Pelland, G. Galanis, and G. Kallos, "Solar and photovoltaic forecasting through post-processing of the Global Environmental Multiscal numerical weather prediction model". *Progress in Photovoltaics: Research and Applications* vol. 21:3 pp. 284–296 2011
- [8] J. Shi, W. Lee, Y. Lee, Y. Yang and P. Wang, "Forecasting power output of photovoltaic systems based on weather classification and support vector machines". *IEEE Transactions on Industry Applications* vol. 48:3 pp. 1064–1069 2012
- [9] J. G. Da Silva Fonseca, T. Oozeki, T. Takashima, G. Koshimizu, Y. Uchida, and K. Ogimoto, "Use of support vector regression and numerically predicted cloudiness to forecast power output of a photovoltaic power plant in Kitakyushu, Japan" *Prog. Photovolt. Res. Appl.* vol.20, pp. 874–882, 2012
- [10] M. Diagne, M. David, P. Lauret, J. Boland and N. Schmutz, "Review of solar irradiance forecasting methods and a proposition for small-scale insular grids", *Renewable and Sustainable Energy Reviews*, vol. 27, pp 65–76, November, 2013.
- [11] E. Lorenz, A. Hammer, D. Heinemann D., "Short term forecasting of solar radiation based on satellite data". *EUROSUN2004 (ISES Europe Solar Congress) 2004:841-8.*
- [12] C. W. Chow, B. Urquhart, M. Lave, A. Domingues, J. Kleissi, J. Shields, and B. Washom "Intra-hour forecasting with a total sky imager at the UC San Diego solar energy testbed", *Solar Energy* vol. 85:11, pp. 2881–2893 2011
- [13] M. Starke, J. Nutaro, T. Kuruganti and D. Fugate, "Integration of photovoltaics into building energy usage through advanced control of rooftop unit", *International High Performance Buildings Conference, Purdue*, 2014
- [14] <http://weather.gc.ca> Access date: July, 1, 2015.
- [15] I. Reda, A. Andreas, A. "Solar position algorithm for solar application." NREL, Technical Report, 2003
- [16] <http://wunderground.com> Access date: July, 1, 2015.
- [17] M. G. Villalva, J. R. Gazoli, E. R. Filho, "Modeling and circuit-based simulation of photovoltaic arrays", *COBEP 09 Power Electronics Conference*, vol. 27, pp 1244–1254, Sep 27 2009- Oct 1 2009.
- [18] A.D. Jones, C.P. Underwood, "A thermal model for photovoltaic systems", *Solar Energy*, vol.70:4 pp. 349–359 2001.